Journal of Alloys and Compounds 525 (2012) 137–142

Contents lists available at SciVerse ScienceDirect

Journal of Alloys and Compounds

journal homepage: www.elsevier.com/locate/jallcom

Effect of particle additions on microstructure evolution of aluminium matrix composite

Katarína Ďurišinová*, Juraj Ďurišin, Mária Orolínová, Martin Ďurišin

Institute of Materials Research of Slovak Academy of Sciences, Watsonova 47, 040 01 Košice, Slovak Republic

ARTICLE INFO

Article history:
Received 9 December 2011
Received in revised form 8 February 2012
Accepted 13 February 2012
Available online xxx

Keywords:
Aluminium alloy
Dispersion strengthening
Microstructure
Powder metallurgy
Thermal stability

ABSTRACT

The study investigates the influence of different fractions of particles (1, 2.5, 5, 8 and 10 vol.%) on microstructure of the as-extruded Al–Al_4C_3 composite as well as on the microstructure evolution at elevated temperatures and after cooling to room temperature. The results indicate that all the materials exhibit a stable microstructure up to 500 °C. The excellent thermal stability is secured by the dispersed nano-particles that strengthen crystallite/grain boundaries by direct interaction of the particles with moving dislocations. In addition, the higher particle contents (8 and 10 vol.%) help to suppress the deformation texture of the hot extruded solids and refine the matrix microstructure to a nanometric scale resulting in a marked enhancing of dislocation density and consequently hardness.

1. Introduction

Aluminium alloys have been considered as high performance materials in automotive and aerospace industry, where damage tolerance is essential. However, commercial aluminium alloys lose their strength and become unusable for structural applications at temperatures above 200–300 °C depending on their composition. From the point of view, much attention has been devoted to developing modern aluminium materials operating at elevated temperatures up to 500 °C [1].

Dispersion strengthening is an important method of improving the strength of aluminium alloys. Thermodynamically stable, non-shearable and fine (<50 nm) particles—dispersoids homogeneously distributed inside the matrix grains and at grain boundaries can contribute significantly to stabilization of the microstructure and strengthen material by an attractive direct interaction of the particles with moving dislocations [2,3]. The dispersoids can impart useful strength to the matrix even at high temperatures, where other strengthening mechanisms (e.g. precipitation hardening) rapidly lose their effectiveness [3]. An appropriate method of including the finest dispersoids into aluminium matrix is the processing technique via high energy milling of powder mixture with subsequent hot extrusion [1,4,5]. Applying the powder metallurgy route of composite materials production makes it possible to establish a thermal stable, fine-grained microstructure with uniform dispersion of small, hard reinforcement particles and hence to obtain optimum properties.

The main aim of the work is to investigate the influence of different volume fractions of dispersoids on microstructure evolution of the Al–Al_4C_3 alloy at room temperature and elevated temperatures up to 500 °C. The composite material was prepared by powder metallurgy techniques and hot extrusion.

2. Materials and methods

The experimental mixtures were prepared by mechanical alloying. Aluminium powder with particle size below 50 μm was dry milled in a Netsch attritor for 90 min with the addition of graphite. The intense milling results in a matrix with fine controlled microstructure and uniform distribution of C particles in as-milled granulates. The granulates were cold pressed in die at 600 MPa into a cylindrical shape and annealed at 550 °C for 30 h in a protective atmosphere to react C to form desired Al_4C_3. In this way were produced Al–Al_4C_3 alloys containing 1, 2.5, 5, 8 and 10 vol.% of dispersoids. The volume fraction of carbide particles in the sample was verified by gas chromatography technique. The cylinders were hot extruded at 600 °C with 94% reduction of the cross section. Extruded bars of 3 mm diameter reach nearly theoretical density. Samples prepared from the bars in the longitudinal and transverse directions, with respect to the direction of extrusion, were investigated regarding their microstructure as a function of the different volume fractions of Al_4C_3 particles and the thermal treatment.

The overall microstructure was observed by Olympus GX 71 light microscope. The microstructure changes of the Al–Al_4C_3 composites were analysed by transmission electron microscopy (TEM) (Tesla BS 500, 90 kV), as well as X–ray diffraction (XRD) (Philips X'Pert Pro diffractometer, 40 kV, 50 mA, Cu Kα radiation). TEM provides a direct picture of microstructure from an area of the thin foil of approximately 1 μm^2. Advantage of the XRD technique over the TEM is in its ability to analyze volume average structural information from much large area of the sample. XRD line broadening is known to be influenced by the microstructure of crystalline solids and the line profile analysis is really a valuable technique for a characterisation in

* Corresponding author. Tel.: +421 55 7922467; fax: +421 55 7922408.
E-mail address: kdurisinova@imr.saske.sk (K. Ďurišinová).

0925-8388/$ – see front matter © 2012 Elsevier B.V. All rights reserved.
doi:10.1016/j.jallcom.2012.02.098

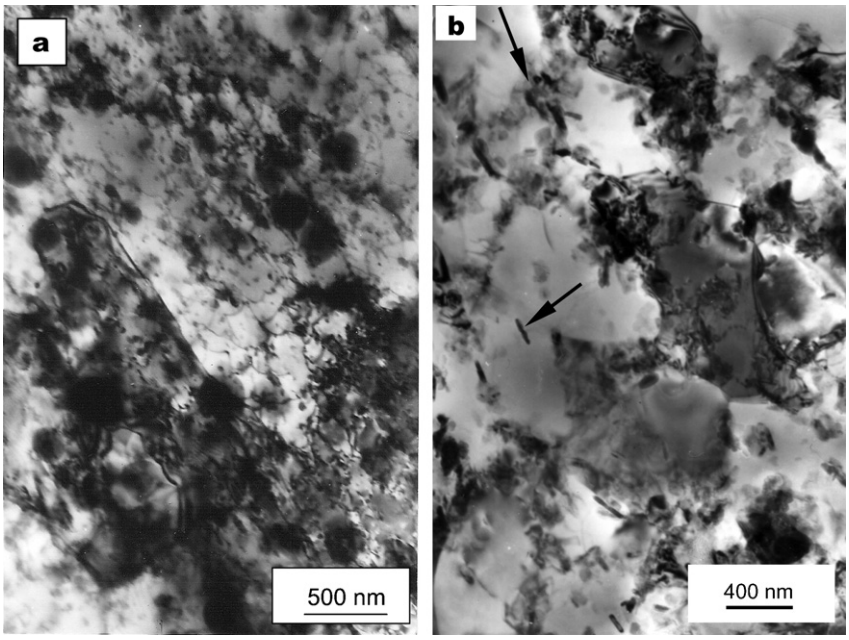

Fig. 1. TEM micrographs of the as-extruded microstructure (longitudinal cross section) at room temperature: (a) Al–1 vol.% Al_4C_3 and (b) Al–10 vol.% Al_4C_3.

terms of size and morphology of crystallites and imperfections in the crystallites (micro-strains, dislocations, stacking faults, etc.). The diffraction lines are broadened when the grain sizes are in the nanometer ranges [6] and the smaller the grain/crystallite sizes the broader the lines. Analysis of the strain broadening of the peak profiles makes it possible to determine the microstrain parameters and the dislocation density calculation. In dispersion strengthened materials, the dislocation density evaluation is important because the direct interaction of particles with moving dislocations is a dominant feature of the microstructure. The strain and mean crystallite/grain size D and the dislocation density ρ in the Al–Al_4C_3 were defined by applying the Williamson–Hall plot [7] and Williamson–Smallman relation [8], respectively. The XRD pattern analyses were used also for identification of matrix and secondary compounds. Extraction of the dispersoids as replicas was done for size distribution and morphology investigation of the particles, as well as for analysis of their composition by electron diffraction from selected area (SAED). The TEM samples were prepared using routine methods applicable to aluminium alloys.

The microstructural evolution was tested by XRD during temperature treatment at 20, 100, 200, 300, 400 and 500 °C, respectively. X-ray diffractograms of the materials were carried out on a Philips X'Pert Pro diffractometer equipped with Cu cathode at operating parameters of 40 kV and 50 mA using the positional sensitive detector X'Celerator and the high-temperature camera up to 1600 °C allowing measurements in situ during thermal exposure of sample. In this experiment, the aluminium crystallite/grain size D was determined by the Voigt function [9] that was used for the detailed analysis of the integral breadths of broadened (1 1 1), (2 0 0) and (2 2 0) diffraction line profiles.

Structural stability was investigated also indirectly, by means of hardness measurements at room temperature according to Vickers (HV 10) on materials pre-annealed at different temperature from 100 to 500 °C for 1 h. It is well known, that material loses its hardness with a microstructure coarsening. The temperature at which the hardness starts to fall down is typically connected to beginning of the recrystallization processes.

3. Results and discussion

3.1. Effect of particle additions on microstructure of as-extruded material

Metallographic observations using light microscopy document a microstructure with poorly visible grain boundaries. The secondary particles are homogeneously distributed in the aluminium matrix in the transversal cross section and those are arranged into parallel rows in the longitudinal direction to the direction of hot extrusion. From TEM analysis can be seen that the Al–1 vol.% Al_4C_3 alloy consists of a fine elongated grain structure parallel to the applied stress during extrusion and approximately equiaxed grains in the transverse cross section. The preferential grain orientation testifies to the deformation texture formation. The grain boundary sliding occurring by dislocation mechanisms, which plays a dominant role during plastic deformation, is not sufficiently suppressed by the dispersoids due to their low content/clustering; the material is characterised by a higher degree of plasticity and consequently the texture rises easily during densification. This kind of microstructure was noted also in the alloys with 2.5 and 5 vol.% of Al_4C_3. A typical TEM microstructure is recorded in Fig. 1(a). Complex dislocation structures characteristic of a heavily deformed material are evident in many areas. The elongated grains in the longitudinal cross sections are often fragmented into a cell substructure that is either incipient in a region with the particle/dislocation interactions or occasionally well defined as a result of recovery processes in the particle-free area. On the contrary, no preferential grain orientation is observed in the alloys with 8 and 10 vol.% of Al_4C_3, grains are there approximately equiaxed and similar in both cross sections, Fig. 1(b). The dislocation sliding is limited in this both materials during the hot extrusion due to effective dislocations movement suppression by higher additions of the fine particles at the grain/subgrain boundaries. A mutual sliding of the grains is also limited, therefore it seems, that the prevailing mechanisms of plastic deformation include a displacement of the whole grains by rotation connected with the restricted grain shape accommodation [10]. In our previous reports [11,12], there are detailed studies on influence of the particles amount on the texture development of the as-extruded aluminium alloy.

Fig. 2 shows the microstructure evolution of the aluminium matrix expressed by changes of the mean crystallite size D and dislocation density ρ depending on the volume fraction of the strengthening particles. By the XRD profile analysis was determined that the crystallite/grain size has values between 76 and 125 nm and the dislocation density ranges from 0.7×10^{14} to 3.0×10^{14} m^{-2}. Fig. 2 presents that when the amount of the dispersoids increases, the crystallite sizes reduce and the dislocation density rises. A marked increasing the dislocation density at the volume fractions of 5, 8 and 10% compared to that in the material with 1 and 2.5 vol.% of particles is associated with a higher number of dislocations anchoring to carbide particles, as well as with the aluminium crystallite sizes in a nanometric scale (<100 nm). The higher volume fractions of particles refine the matrix

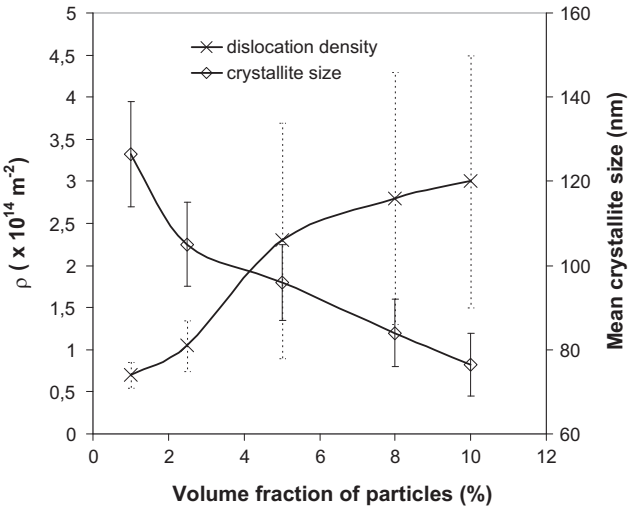

Fig. 2. Microstructure evolution of the aluminium matrix expressed by changes of the mean crystallite size D and dislocation density ρ depending on the volume fraction of the Al_4C_3 particles.

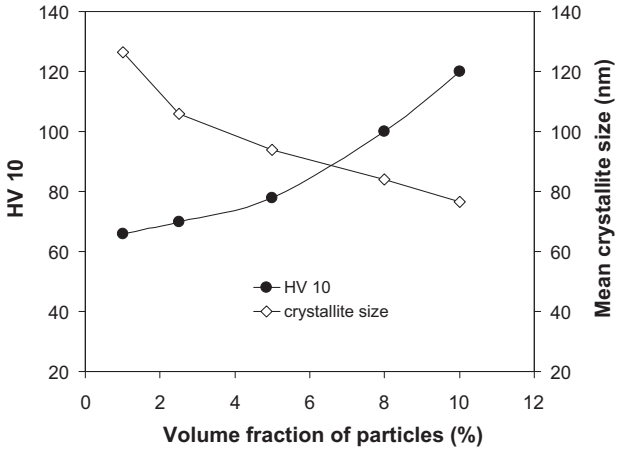

Fig. 3. Vickers hardness and mean crystallite size as a function of the volume fraction of the Al_4C_3 particles.

microstructure due to a more marked retardation of the recrystallization processes occurring during hot extrusion at 600 °C. These dispersoids block the cross slip and both the strain and thermally activated movement of dislocations effectively resulting in an ultrafine non-textured microstructure formation. The grain/subgrain structure is not completely developed in the alloys containing 8 and 10 vol.% of Al_4C_3, but mostly consists of diffuse, poorly defined boundaries, as can be clearly seen in Fig. 1(b). On the other hand, the cell substructure of the alloy with 1 vol.% of dispersoids observed by TEM is well noticeable in Fig. 1(a). The cell size is in accordance with the crystallite size measured by XRD.

Fig. 3 documents that the measured Vickers hardness (HV 10) at room temperature grows with increasing the volume fraction of particles and decreasing the aluminium crystallite size. A significant enhancement in the hardness takes place at the highest additions of 8 and 10 vol.% of particles where the mean crystallite sizes reach the minimum values of 84 and 76.5 nm, respectively. Almost the 2-times increased hardness of the Al–10 vol.% Al_4C_3 (HV = 120 at D = 76.5 nm) against that in the Al–1 vol.% Al_4C_3 (HV = 66 at D = 126.5 nm) results from its nanostructure in the area below 100 nm which significantly improves mechanical properties compared to the coarse-grained counterparts.

Phase analysis performed on the XRD patterns from the Al–Al_4C_3 alloys proved apart from Al crystals the presence of aluminium carbide confirming the required transformation of the initial C after finishing of the material preparation. The SAED patterns of replicas from the composites in Figs. 4 and 5 showed that the particles consist of Al_4C_3. The SAED patterns adherent to Al_4C_3 are ring type, which reveal the random and fine structure of polycrystalline grains of the dispersoids. In some areas there was identified also γ-Al_2O_3 phase. The Al_2O_3 was formed during the powder processing due to a high affinity Al to O_2. However, its fraction is low, about 1 vol.%. The TEM images of replicas in Figs. 4 and 5, as well as directly TEM observations of thin foils in Fig. 1 illustrate that the carbide dispersoids in the material with 10 vol.% of Al_4C_3 are primarily isolated individual particles or clusters of few particles whereas in the material with 1 vol.% of Al_4C_3 there exist single particles and also occasional clusters. The effective dispersoid size was determined to be approx. 30 nm. The carbide particles are either needle-shaped, as it is documented by arrows in Fig. 1(b), or spheroidal ones. The fine dispersoids are located mostly at the grain/subgrain boundaries, and dislocations commonly interact with them what is a fundamental microstructure feature of these dispersion strengthened alloys. The microstructure impurities such as Al_2O_3 phase represent coarser particles with size around 500 nm approximately of a spherical morphology. The strengthening potential of the coarse particles and larger clusters is insignificant at elevated temperatures.

3.2. *Effect of particle additions on microstructural development at elevated temperatures*

Fig. 6 shows TEM micrographs of a longitudinal cross section of the as-extruded composites with 1 and 10 vol.% of Al_4C_3 after 1 h

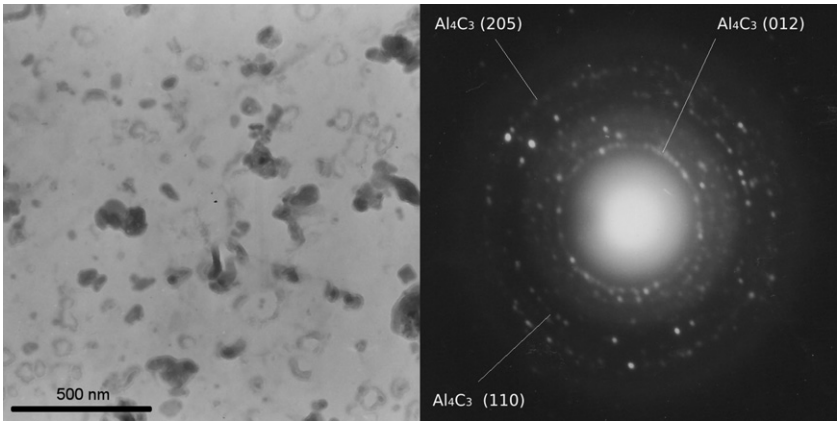

Fig. 4. TEM picture of particles in extraction replica of Al–1 vol.% Al_4C_3 alloy and corresponding SAED pattern.

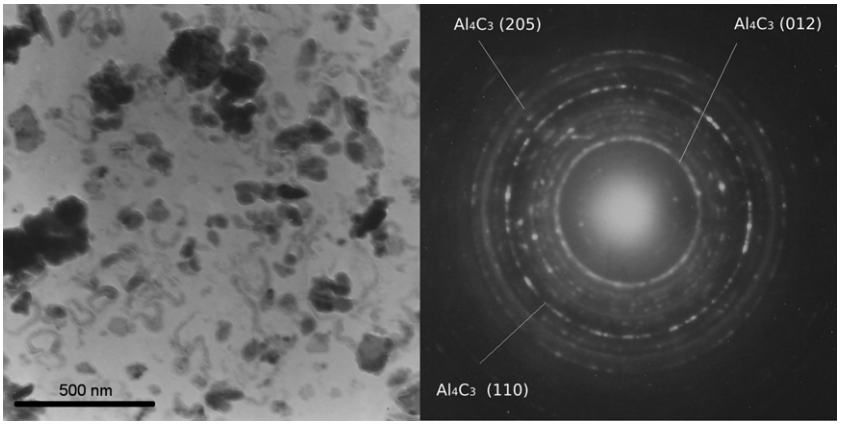

Fig. 5. TEM picture of extraction replica showing the size distribution and morphology of the particles, as well as particle clustering in Al–10 vol.% Al_4C_3 alloy and corresponding SAED pattern.

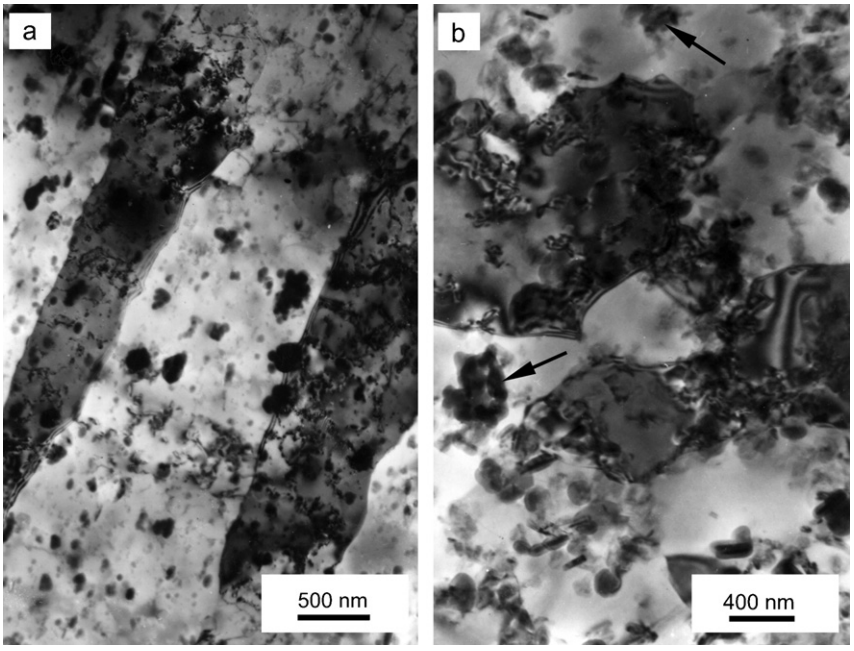

Fig. 6. TEM micrographs of the as-extruded microstructure (longitudinal cross section) annealed at 500 °C for 1 h: (a) Al–1 vol.% Al_4C_3 and (b) Al–10 vol.% Al_4C_3.

heat treatment at 500 °C in argon atmosphere. The pre-annealed material containing 1 vol.% of Al_4C_3 exhibits a minimal change of the matrix grains, as well as the size and distribution of secondary phases and no microstructure changes were observed in the material with 10 vol.% of Al_4C_3 as compared to the initial state at room temperature (see Fig. 1). The XRD results of the mean crystallite sizes on the (1 1 1) slip plane in Fig. 7 confirm that only a minor or negligible growth of the initial crystallite size is evident in the materials containing 1, 2.5 and 5 vol.% Al_4C_3 and no crystallite growth occurs in the Al–10 vol.% Al_4C_3 after cooling of the samples from 500 to 20 °C (see also Table 1). This feature can be explained by the influence of thermal stresses arising at the interphase boundaries during cooling due to a difference between the thermal expansion coefficient (CTE) of the matrix and the particle (CTE_{Al} = 23.5 to 26.5 × 10^{-6} K^{-1} and CTE_{Al4C3} = 5 × 10^{-6} K^{-1}). This difference causes the misfit strains at the interface and induces thermal stresses. When the stresses reach a certain level, a generation of the new dislocations accumulating at the barriers–particles results in the stress relaxation what can enhance the dislocation density and subsequent recreating small crystallite/grains during cooling to room temperature. The plastic deformations due to the CTE mismatch caused no microcracks at the interfaces between the reinforcing particles and the matrix.

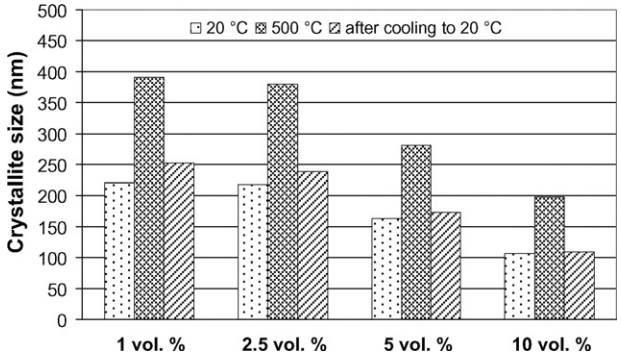

Fig. 7. The aluminium crystallite size on the (1 1 1) slip plane after cooling of the samples from 500 to 20 °C compared to the initial state at room temperature at different volume fraction of Al_4C_3 particles.

Structural stability of the as-extruded materials containing 1, 2.5, 5, 8 and 10 vol.% of dispersoids was tested also by means the

Table 1
Aluminium crystallite size D for Al–Al_4C_3 materials at different temperatures and its relative change D_{rel} ($D_{rel} = D_{500} - D_{20}/D_{20}$).

$h\,k\,l$	Temperature (°C)							D_{rel} (%)
	20	100	200	300	400	500	20 cool[a]	
	Crystallite size D (nm)							
Al–1 vol.% Al_4C_3								
(1 1 1)	220.5	231.6	275.2	332.8	366.0	391.6	252.5	77.6
(2 0 0)	129.9	148.6	165.2	224.2	227.7	251.2	146.4	93.4
(2 2 0)	82.8	85.6	111.2	131.4	166.1	193.0	76.8	133.0
Al–10 vol.% Al_4C_3								
(1 1 1)	106.7	128.0	150.9	167.9	187.4	197.8	108.7	85.4
(2 0 0)	94.3	104.1	111.0	147.6	174.0	190.1	75.9	102.0
(2 2 0)	65.6	84.6	99.6	130.1	169.2	191.7	64.4	192.2

[a] After cooling of the sample from 500 to 20 °C.

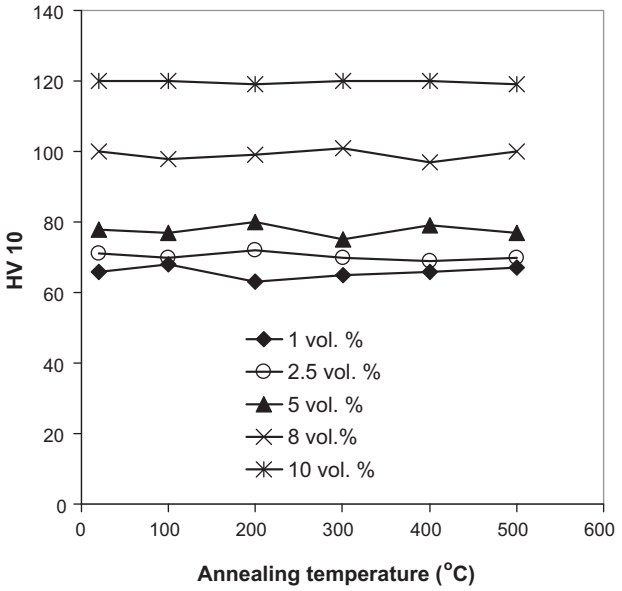

Fig. 8. Hardness of the Al–Al_4C_3 materials after 1 h annealing at different temperatures.

Vickers hardness as a function of the annealing temperature from 100 to 500 °C for 1 h, Fig. 8. The measurements confirm that all the materials exhibit no hardness changes after the annealing and quenching to room temperature, suggesting thermal stability of the microstructure over the probed temperature range. This conclusion is in good agreement with the TEM and XRD analyses.

By in situ XRD the microstructure evolution was tested for the materials with 1 and 10 vol.% of particles during temperature treatment at 20, 100, 200, 300, 400 and 500 °C, respectively, and results are summarized in Table 1. The results of the line profile analysis show that a crystallite size growth is observed in all diffraction planes at the increasing temperature due to the softening of the matrix. The thermally activated dislocations motion induces in the both experimental materials a collective rearrangement and annihilation of dislocations resulting in dynamic recovery process. The grains have a low concentration of lattice defects reflecting in a crystallite coarsening with the increasing temperature, Table 1. In addition, the thermal stresses derivable from CTE mismatch can reach values up to the matrix yield stress at the temperature of 500 °C causing micro-shear of newly developed dislocations. The stresses act in directions from the grain/subgrain boundaries (places where particles or clusters are located) towards the centre of the grains [13]. In small grains, dislocations induced at the grain boundaries can annihilate by moving against to each other on slip planes. As can be seen from the results in Table 1, relative crystallite size changes D_{rel} ($D_{rel} = D_{500} - D_{20}/D_{20}$) of Al–1 vol.% Al_4C_3 are lower than these ones in the Al–10 vol.% Al_4C_3. This unexpected behaviour of the material containing the higher volume fraction of particles could be interpreted by reduced thermal stability of the initial nanometric grains, which promote annihilation of dislocations, compared to a coarser, more equilibrium grains in the Al–1 vol.% Al_4C_3. However, the final crystallite size at 500 °C there is finer in all diffraction planes than that in Al–1 vol.% Al_4C_3 material. The study showed that the higher addition of particles strengths the aluminium nano-grains at elevated temperatures resulting in abnormal grain growth retardation. As can be seen, dispersion hardening comes across as a potent strengthening mechanism for improving thermal stability of nano-grains. The creep rate of the particle-strengthened system is reduced because a dislocation surmounting a dispersoid generally encounters two barriers: the “climb barrier” and the “detachment barrier”, which prevents the dislocation from leaving the particle [2,3]. Compared with dispersoid-free material, the deformation of strengthened alloys is largely controlled by microstructural constraints on dislocation or vacancy motion.

One may conclude from the discussion above that improvement in both the microstructure refining to a nanoscale region and texture development suppression can be obtained by enhancing the volume fraction of strengthening particles. The thermal microstructural stability is sufficient over the all particle contents that means also at the lowest addition of 1 vol.%. It is of interest to use uniformly distributed nano-sized particles to strengthen the aluminium matrix, while maintaining good ductility and high creep resistance. However, the ductility deteriorates significantly with high particle concentration. As can be seen from TEM observations, the agglomerations of the Al_4C_3 particles are visible in many areas of the matrix. The strengthening effect of the coarse particles and larger clusters is insignificant at elevated temperatures. Thus, substantial reduction in the carbide content at their homogeneously dispersion should be feasible without seriously impairing the potential strengthening benefits. The improvement may be achieved by designing the processing route to obtain the optimum microstructures at an addition likely below 3 vol.% of the particles into the aluminium matrix. Future work will examine the mechanical behaviour of these materials.

4. Conclusion

The results obtained by the study led to the following conclusions:

1. The as-extruded composite microstructure consists of fine-grained aluminium matrix strengthened by dispersed nanometric Al_4C_3 particles. The fine particles interacting with dislocations are a characteristics feature of the microstructure.

2. The higher particle contents (8 and 10 vol.%) help to suppress the formation of deformation texture in the hot extruded solids and refine the microstructure to a nanometric scale resulting in the marked enhancing of dislocation density and hardness.
3. The materials over the all particle additions show a minor/no mean crystallite size and hardness changes after the annealing, suggesting microstructural stability up to 500 °C. The excellent thermal stability is secured by the dispersed nano-particles that strengthen grain boundaries and retard the recrystallization and grain growth at elevated temperatures by direct interaction of the particles with moving dislocations. Also the dislocations generated by thermal mismatch contribute to the matrix strength.
4. The initial crystallite sizes of the both composites with 1 and 10 vol.% of particles grow about linearly at increasing temperatures of 100, 200, 300, 400 and 500 °C, respectively. However, no abnormal grain growth takes place because there the creep rate of the system is reduced by microstructural constraints – fine particles on dislocation or vacancy motion.
5. A lot of the particles is transformed into unwanted coarser agglomerates during preparation/compaction of the powder alloy. The improvement could be achieved by designing the processing route to obtain an optimum microstructure at a lower addition of the particles (likely under 3 vol.%) in the aluminium matrix.

Acknowledgement

The authors are grateful to the Scientific Grant Agency of the Ministry of Education of Slovak Republic and the Slovak Academy of Sciences (VEGA Project No. 2/0167/10) for the financial support of this work.

References

[1] K.I. Moon, K.S. Lee, J. Alloys Compd. 291 (1999) 312–321.
[2] J. Rösler, Int. J. Mater. Prod. Technol. 18 (2003) 70–90.
[3] E. Arzt, G. Dehm, P. Gumbsch, O. Kraft, D. Weiss, Prog. Mater. Sci. 46 (2001) 283–307.
[4] M. Adamiak, J. Achiev. Mater. Manuf. Eng. 31 (2008) 290–293.
[5] R. Deaquino-Lara, I. Estrada-Guel, G. Hinojosa-Ruiz, R. Flores-Campos, J.M. Herrera-Ramírez, R. Martínez-Sánches, J. Alloys Compd. 509S (2011) S284–S289.
[6] H.P. Klug, L.E. Alexander, X-ray Diffraction Procedures for Polycrystalline and Amorphous Materials, J. Wiley & Sons, New York, 1974.
[7] G.K. Williamson, W.H. Hall, Acta Metall. 1 (1953) 22–31.
[8] G.B. Williamson, R.C. Smallman, Philos. Mag. 1 (1956) 34.
[9] T.H. de Keijser, J.I. Langford, E.J. Mittemeijer, A.B.P. Vogels, J. Appl. Crystallogr. 15 (1982) 308–314.
[10] M. Besterci, O. Velgosová, F. Lofaj, L. Kováč, Metalurgija 44 (2005) 255–259.
[11] J. Ďurišin, M. Orolínová, K. Ďurišinová, M. Besterci, Kov. Mater. Met. Mater. 45 (2007) 269–274.
[12] M. Orolínová, J. Ďurišin, K. Ďurišinová, M. Besterci, K. Saksl, High Temp. Mater. Process. 28 (2009) 73–81.
[13] Z. Trojanová, P. Lukáč, H. Ferkel, W. Riehemann, B.L. Mordike, Kov. Mater. Met. Mater. 37 (1999) 8–17.